Karakoc, Alp; Freund, Jouni

A statistical failure initiation model for honeycomb materials

Published in:
Composite Structures

DOI:
10.1016/j.compstruct.2012.07.001

Published: 01/01/2013

Document Version
Peer-reviewed accepted author manuscript, also known as Final accepted manuscript or Post-print

Please cite the original version:
Karakoc, A., & Freund, J. (2013). A statistical failure initiation model for honeycomb materials. *Composite Structures*, (95), 154-162. https://doi.org/10.1016/j.compstruct.2012.07.001

A STATISTICAL FAILURE INITIATION MODEL FOR HONEYCOMB MATERIALS

Alp Karakoç*, Jouni Freund

Aalto University, School of Engineering, Department of Applied Mechanics, P.O.BOX 14300, FI-00076 AALTO, FINLAND

ABSTRACT

In the current study, a statistical failure initiation model for honeycomb materials is proposed. The model describes the failure initiation in macroscopic normal-shear stress space. The workflow of the model is explained in three stages: micromechanical model, simulation experiments under external macrostresses and boundary conditions, and analysis of the experiment results. In the micromechanical model, the heterogeneous nature of the material is described with the geometrical parameters which are irregularity and scale, and their variations. Based on these parameters, samples are designed and simulation experiments are conducted. The experiment results are linked to possible failure mechanisms in order to obtain the critical macroscopic stresses which are expressed in terms of cumulative distribution functions. Further investigations on these functions with the weakest link theory and Weibull distribution lead to understand and quantify the effects of the geometrical parameters on the failure initiation characteristic in a statistical manner. As a result of these investigations, the statistical model describing the failure initiation of honeycomb materials is presented as functions of the irregularity and scale in macroscopic stress space.

Keywords: Failure initiation, honeycomb, micromechanical, cumulative distribution, the weakest link, Weibull distribution.

---

*Corresponding author. Tel: +358 470 23442.

Email address: alp.karakoc@aalto.fi (Alp Karakoç).

1. INTRODUCTION

Honeycomb materials are widely used for various structural applications due to the minimized amount of material usage and high stiffness-to-weight ratios [1]. They can easily function as tailored solutions for different special problems due to their design as interconnected network of solid struts. Since being a popular material in engineering applications, there have been studies related to their deformation and failure mechanisms in the literature. These include the research activities on the elastic properties of regular honeycombs for which the struts form equilateral cells with exactly the same corner angles [2-4]. Such analyses are not, however, feasible since they do not take the microstructural variations into account [5]. This necessitated developing models for irregular honeycombs which have random deviations in shape and size of their cell structures [6, 7]. Although the effects of irregularities and imperfections on the elastic and failure properties have been wisely modelled, the results have been mostly analysed in deterministic manner [8]. However, taking heterogeneous nature of the honeycomb materials into consideration, more realistic results can be obtained by blending these micromechanical models with statistical analysis techniques [9].

In order to complete this missing link in the literature, the proposed model, which is an extension of the conference articles [10, 11], aims at expressing the effects of geometrical parameters such as irregularity and scale on the failure initiation of the honeycomb materials in a compact, statistical form. The present investigation starts with a micromechanical model for honeycomb materials which explains the geometrical and mechanical relations separately. In this micromechanical model, the heterogeneous nature of the material is described with the geometrical parameters such as irregularity and scale and their variations. Based on these parameters, samples are designed and simulation experiments are conducted. The experiment results are linked to possible failure mechanisms to obtain the critical macroscopic stresses and analyze the effects of irregularity and scale in terms of statistical methods. The outcome of the analysis is the generic cumulative distribution function in macroscopic stress space describing the failure initiation probabilities of the honeycomb materials.

2. OVERVIEW

2.1. Objectives

The main objective of the present study is to develop a statistical failure initiation model for honeycomb materials in macroscopic stress space. The model is designed so that once the failure initiation statistics of a reference honeycomb sample is known for a specific macrostress combination, it is possible to predict the failure initiation statistics for honeycombs of various geometrical features and scales under the same macrostresses. For a convenient representation, the failure initiation statistics is described in terms of cumulative distribution function which gives the probability with which a material fails under the critical macrostress value. As a result of this study, the critical macrostress limits and failure initiation probabilities of the honeycomb materials can be obtained and catastrophe can be avoided well in advance.

2.2. Statistical failure initiation model

In order to form the statistical failure initiation model, experiments are carried out under various external macrostress combinations $\underline{\mathbf{s}}$ for both regular honeycombs composed of equilateral cells with same corner angles and irregular honeycombs with variations in cell sizes and corner angles. Thereafter, the experiment results are linked to possible failure mechanism(s) and the critical macrostress values $\mathbf{s}_{cr}$ are calculated and plotted in a chosen stress space, e.g. macroscopic normal-shear stress space, as illustrated in Fig. 1. Since $\mathbf{s}_{cr}$ is unique for regular honeycombs under each stress combination and is independent of size of the material, the outcome is always a curve defining the maximum possible safe region. If this curve is exceeded, the failure initiation is unavoidable. In case of irregular honeycomb(s) of irregularity α and scale $\underline{V}$, the phenomenon is explained with a variation domain instead of a curve. As shown in Fig. 1, the variation domain can be described in terms of cumulative distribution function which gives the probability with which a material fails under $\mathbf{s}_{cr}$. By using necessary statistical tools and cumulative distributions, it is possible to describe the variation domain for wide range of α and $\underline{V}$.

---Preferred position for Fig. 1---

2.3. Methodology

In order to describe the variation domain and understand the effects of the parameters on the failure initiation, samples of various α and $\underline{V}$ should be tested either physically or virtually. However, it is a very challenging task to carry out physical experiments due to the need for excessive amount of data. Therefore, the present study focuses only on simulation experiments. For this purpose, a micromechanical model is developed as shown in Fig. 2. By means of this model, both microscopic and macroscopic mechanical field quantities are calculated under different $\underline{\mathbf{s}}$ and boundary conditions. Then, the failure mechanism(s) to be used is decided, e.g. bending moment can be taken to be decisive for failure due to its dominance on cell wall deformation of the honeycombs. In the following step, the critical bending moment M_{cr} and the critical macrostress $\mathbf{s}_{\mathrm{cr}}$ causing the first beam to fail are linked to each other in terms of maximization and scaling operations. Then, $\mathbf{s}_{\mathrm{cr}}$ values for honeycombs of different α and $\underline{V}$ are analyzed by using statistical tools such as the weakest link and Weibull theories. The outcome of the analysis is the generic cumulative distribution function which describes the failure initiation probabilities of the honeycomb materials.

---Preferred position for Fig. 2---

3. MICROMECHANICAL MODEL

The current micromechanical model represents the honeycomb material as a heterogeneous medium where the errors related to homogenization and discretization can be eliminated by direct calculations for the microscopic mechanical quantities [12]. The following subsections explain this modeling approach in detail.

3.1. Material element

The material element is a $H \times H$ square honeycomb as seen in Fig. 3. The independent geometrical variables are the measure of geometrical irregularity α and the dimensionless scale parameter $\underline{V} = \left(H/h^0\right)^2$, where H is the specimen size and h^0 is the cell wall height for the regular honeycomb material. The measure of irregularity α is the ratio between the cell wall height offset Δh and h^0 as shown in Fig. 3. Here, the regularity of the material is described by a one-parameter model, in which $\alpha = 0$ and $\alpha > 0$ correspond to regular and irregular material geometries, respectively. To be more precise, the cell vertices are given random offsets of magnitude $\Delta h = \alpha h^0$ and the uniform distribution interval is determined as $[h^0 - \Delta h, h^0 + \Delta h]$. However, the scale $\underline{V} = \left(H/h^0\right)^2$ is treated in a deterministic way, while the shapes and sizes of the cells, cell wall elastic modulus E_s and thickness t of the cell walls are assumed to be known.

In the laboratory *XY*-coordinate system, the domain occupied by the specimen is $\Omega = [0,H]\times[0,H]$, where $\partial\Omega$ represents the boundary domain.

---Preferred position for Fig. 3---

3.2. Beam equations

In the micromechanical model, the cell walls of Fig. 3 are modeled as elastic Bernoulli beams. The material inside the cells is taken to be soft compared to that of the walls. In this beam model, the equilibrium equations in beam *xyz*-Cartesian coordinate system are

$$\vec{F}' + \underline{\vec{f}} = 0\,, \tag{1}$$

$$\vec{M}' + \vec{i} \times \vec{F} + \underline{\vec{m}} = 0\,, \tag{2}$$

in which unit vectors $\vec{i}, \vec{j}, \vec{k}$ are codirectional with *x*-, *y*-, and *z*-axes. The prime symbol is used to denote the derivative with respect to *x*. In Eqs. (1) and (2), $\underline{\vec{f}}$ and $\underline{\vec{m}}$ are the external load parameters, and $\vec{F}$ and $\vec{M}$ are the stress resultants acting on a beam cross-section. The constitutive equations for $\vec{F}$ and $\vec{M}$ of a linearly elastic material take the forms

$$\vec{F} = (E_s A u_x')\,\vec{i} - \left(E_s I u_y'''\right)\vec{j}\,, \tag{3}$$

$$\vec{M} = (E_s I u_y'')\,\vec{k}\,, \tag{4}$$

in which u_x, u_y are the displacement components in the directions of the *x*- and *y*-axes. Elastic modulus E_s is the constant material parameter of the problem. The geometrical properties of beam cross sections are $A = \mathcal{T} t$ and $I = \mathcal{T} t^3 / 12$ in which t is the cell wall thickness which is same as the beam depth and $\mathcal{T}$ is the thickness of the honeycomb material which is same as the beam width. The *x*-axis of the *xyz*-coordinate system is assumed to coincide with the neutral axis of the beam.

Solutions to Eqs. (1) and (2) for the cell walls modelled as beams of Fig. 3 are connected by continuity conditions concerning displacements and rotations at vertices and the equilibrium of the vertex points.

3.3. Failure initiation criterion

Failure mechanisms of a honeycomb depend highly on the material details. Identification and modeling of the likely mechanisms are one of the challenges of a simulation experiment design. In the current study, bending moment is assumed to be decisive for the failure initiation considering its dominant effect on the cell wall deformations [1, 13]. Hence, the material is assumed to fail when the bending moment in a beam exceeds the critical bending moment value M_{cr}.

Let us denote the maximal absolute values of the bending moments of the beams with $M_j \quad j \in \{1, 2, \ldots, n\}$, where n is the total number of the beams in Ω. Then, the failure initiation occurs when

$$\max_{j \in \{1,2,..n\}} \left| M_j \right| = M_{\mathrm{cr}}, \tag{5}$$

in which $|\;|$ is the absolute value function. Under linearity assumption, the critical macrostress value $\mathbf{s}_{\mathrm{cr}}$ resulting in the first beam to fail is obtained by scaling

$$\mathbf{s}_{\mathrm{cr}} \equiv p\underline{\mathbf{s}} = \frac{M_{\mathrm{cr}}}{\max_{j \in \{1,2,..n\}} \left| M_j \right|} \underline{\mathbf{s}}, \tag{6}$$

in which p is the linear scaling term.

4. SIMULATION EXPERIMENTS

A simulation experiment on failure initiation is designed similar to a physical one: in order to study the population characteristics, such as strength of an irregular honeycomb material, experiment is repeated on a random sample, and the failure initiation statistics is estimated based on the results of the sample. In the present work, the aim is to understand the effect of independent geometrical variables such as irregularity α and scale $\underline{V}$ on the failure initiation statistics.

4.1. Design of experiments

In these experiments, the effects of α and $\underline{V} = \left(H/h^0\right)^2$ on failure initiation is studied on samples of $j = 500$ specimens. Each sample is generated for $H/h^0 \in \{10, 20, 40, 60\}$, $\alpha \in \{0, 0.03, 0.15, 0.2, 0.3\}$. The dependent variable of the problem is the critical macrostress value of failure initiation $\mathbf{s}_{\mathrm{cr}}$ which is obtained through Eq. (6). Material parameters of the model are assumed to satisfy the condition $E_s I / E_s A h^2 \ll 1$ so that the bending effect in Eqs. (1) and (2) is significant [14].

4.2. Experiments

Simulation experiments on failure initiation are performed with an in-house code written with Mathematica® software package. The microscopic material properties and boundary conditions are assigned to the honeycomb cell walls posterior to the generation of specimen geometries. After this step, experiments are conducted.

In these experiments, three different loading conditions are studied in order to describe the failure initiation curves and variation domains of Fig. 1 with minimal effort. The loading conditions are given in terms of external macrostresses: (I) uniaxial tension, i.e. $\underline{s}_{XX} = s$, $\underline{s}_{XY} = \underline{s}_{YX} = \underline{s}_{YY} = 0$, (II) combined loading, i.e. $\underline{s}_{XX} = \underline{s}_{XY} = \underline{s}_{YX} = s$, $\underline{s}_{YY} = 0$, (III) pure shear, i.e. $\underline{s}_{XY} = \underline{s}_{YX} = s$, $\underline{s}_{XX} = \underline{s}_{YY} = 0$. In the current experiments, the material coordinate system is assumed to coincide with the laboratory coordinate system. However, the transformation rules should be applied when these coordinate systems do not coincide [15].

The boundary condition problems such as artefacts due to loading near the edges and underestimation of strength are minimized by defining boundary and solution domain separately and using structural units instead of individual beam elements [7]. As shown in Fig. 4, the external loading acting on the specimen is taken into consideration in Eqs. (1) and (2) at the ends of these structural units on $\partial\Omega$. Hence, the external load parameter $\underline{\vec{f}}$ acting on the beams is calculated through

$$\underline{\vec{f}} = \mathcal{T}\left(\vec{N} \cdot \underline{\mathbf{s}}\right) \cdot \mathbf{R} \tag{7}$$

in which $\cdot$ is the dot product, $\vec{N}$ is the unit surface normal coinciding with the neutral axis of the beam and $\mathbf{R}$ is the rotation tensor [16]. Eq. (7) is also applicable for $\underline{\vec{m}}$ in case of external moment stresses.

---Preferred position for Fig. 4---

Here, it is also noteworthy to mention that one of the vertices is given zero displacement and rotation in order to have unique solution for Eqs. (1) and (2).

5. ANALYSIS

5.1. Cumulative distribution function for failure initiation

For each sample, the simulation experiments result in a set of scaling terms $P=\{p_1, p_2, \ldots p_j\}$ ($j=500$ specimens) that gives the relationship between the external macrostress $\underline{\mathbf{s}}$ and critical macrostress $\mathbf{s}_{\mathrm{cr}}$ as given in Eq. (6). The scaling term set P for each sample is divided by the constant scaling term p^0 of the regular honeycomb specimen with $\alpha=0$. Hence, $\Pi=\{p_1/p^0, p_2/p^0, \ldots, p_j/p^0\}$ can be formed in order to compare the irregular and regular specimens. These data sets are used to calculate the cumulative distribution function for the failure initiation of the samples with irregularity α and scale $\underline{V}$. Hence,

$$\mathrm{cdf}(p/p^0, \alpha, \underline{V}) = \frac{\left|\{p/p^0 \in \Pi : p_j/p^0 \leq p/p^0\}\right|}{|\Pi|} \tag{8}$$

in which $|\ |$ denotes the size of a set. The cumulative distribution function in Eq. (8) gives the probability with which a specimen fails when the p/p^0 ratio is satisfied. Alternatively, one may think that Eq. (8) gives an estimate for the proportion of the sample failing before p/p^0.

5.2 The weakest link theory

The weakest link theory assumes that the failure initiation of a specimen is determined by its weakest element. According to this theory, the failure of the weakest element produces a local stress peak which triggers the failure of the neighboring element(s) and thereby the entire specimen. It is postulated that the cumulative distributions of the samples with different scales $\underline{V}_1$, $\underline{V}_2$ but the same irregularity α can be connected to each other through

$$1-\mathrm{cdf}(p/p^0,\alpha,\underline{V}_2)=[1-\mathrm{cdf}(p/p^0,\alpha,\underline{V}_1)]^{\underline{V}_2/\underline{V}_1} \quad . \tag{9}$$

Hence, it is enough to measure the failure initiation statistics of only one scale to predict the statistics of the target scale(s). Eq. (9) describes an ideally brittle material which narrows the class of materials to be considered quite effectively [17-19]. In this theory, specimen geometry should be irregular enough so that load can be uniformly shared by the elements of the specimen [20]. As a result of this, the location of the first failing elements is randomized and the distribution of these locations becomes more even within the sample.

5.3. Weibull distribution

In addition to the weakest link theory, three parameter Weibull distribution is the other necessary tool to form the statistical failure initiation model. By means of this distribution, it is possible to fit the cumulative distributions which are represented as data lists. This distribution is formulated as

$$w(p/p^0,\alpha,\underline{V})=1-\exp\left[-\left(\frac{p/p^0-\Pi_{\min}}{\lambda}\right)^{\kappa}\right] \tag{10}$$

in which λ and κ are the scale and shape parameters, respectively [21]. The minimum limit value $\Pi_{\min}$ is locally defined for each sample. However, in order to obtain a generic form of Eq. (10), the global minimum value $\Pi_{\min}^{\mathrm{glob}}$ must be calculated for a sample with very large $\underline{V}$ and α which are physically realistic.

6. RESULTS

In this section, experiment results are explained in detail for the samples under uniaxial tension, i.e. $\underline{s}_{XX}=s$, $\underline{s}_{XY}=\underline{s}_{YX}=\underline{s}_{YY}=0$. The results related to other loading conditions which are combined loading, i.e. $\underline{s}_{XX}=\underline{s}_{XY}=\underline{s}_{YX}=s, \underline{s}_{YY}=0$ and pure shear, i.e. $\underline{s}_{XY}=\underline{s}_{YX}=s, \underline{s}_{XX}=\underline{s}_{YY}=0$, are discussed briefly. Eventually, the statistical failure initiation model is given in a compact form for the tested loading conditions.

6.1. Effects of irregularity and scale on failure initiation statistics

The experiments show that the regular honeycomb specimen with $\alpha = 0$ always displays deterministic behaviour on failure initiation regardless of the scale, giving the maximum possible scaling term p^0. Even, the location of the first failing element in the specimen is always the same spot, regardless of the sample size (here, $j = 500$ specimens). This phenomenon always gives the set $\Pi = \{1, 1, ..., 1\}$, resulting in the global maximum value $\Pi_{\max}^{\mathrm{glob}} = 1$.

In case of near regular honeycombs, e.g. here samples with $\alpha = 0.03$, non-deterministic behavior is expected. However, the experiments show that the first failing elements are located near the boundary region due to oriented geometry and boundary artifacts as seen in Fig. 5. This indicates that load sharing is not uniform. In this situation, estimations for the failure initiation probability can be misleading.

In contrast to the assumption of geometrical regularity, the honeycomb materials have irregular geometries and random distribution of the mechanical properties in nature. Therefore, they are expected to have non-deterministic behaviour. For instance, in case of the failure initiation, the location of the first failing element becomes more random, as the irregularity increases inside the material. The randomness of the weakest element is also observed in the simulation experiments as shown in Fig. 5. However, increasing irregularity causes an important deficiency which is the loss of periodicity. Due to this problem, there occurs to be distortion in the alignment of the beam elements with respect to the loading direction. As a result, especially, the bending moments on some vertices (beam ends) increase rapidly when the specimen is exposed to external loading. Therefore, increased irregularity causes the first element to fail under lower $\underline{\mathbf{s}}$ values [22].

---Preferred position for Fig. 5---

From a probabilistic point of view, there is a close relationship between the scale $\underline{V}$ and the failure initiation. The probability of failure initiation is higher for larger materials compared to smaller scales under the same loading conditions [23, 24]. This is mainly due to the increasing probabilities of the elements with weak mechanical properties in large materials [25]. In case of testing a specimen of extremely large scale $\underline{V}$, this probability reaches its highest practical value. In order to calculate such a hypothetical value, the minimum scaling terms $\Pi_{\min}$ of the samples are fitted with the exponential function

$$f(x) = a\exp(-bx), \tag{11}$$

in which a, b are the unknown coefficients and x is the variable. In Fig. 6, the fitted curves of each scale are extrapolated to compute the values of $\Pi_{\min}$ for the maximum irregularity that is $\alpha = 0.5$. In case of exceeding $\alpha = 0.5$, the beam elements overlap resulting in unrealistic honeycomb geometries. For this extreme case, the trend for $\Pi_{\min}$ of each scale is checked and again extrapolated to find the global minimum value $\Pi_{\min}^{\text{glob}}$ for a practically large scale, e.g. here $\underline{V} = 40000$ (or $H/h^0 = 200$). The $\Pi_{\min}^{\text{glob}}$ values for tested loading conditions vary between 0.17 and 0.18. These values are used to form the generic Weibull distribution of Eq. (10).

---Preferred position for Fig. 6---

As seen in Fig. 7, the increments in α cause the cumulative distribution curves to reach the vertical dashed line on the left hand-side representing $\Pi_{\min}^{\text{glob}}$. The main reason is that the moment/load carrying capacities of the elements decrease due to geometrical distortions. Thus, some of the elements become weaker and the failure initiation probability increases. The curves also show that the increase in both α and $\underline{V}$ results in higher probability of the failure initiation. This close relationship is due to the weakening effect of α on the elements and the augmenting effect of $\underline{V}$ on the probability for the existence of weak elements inside the specimen.

---Preferred position for Fig. 7---

6.2. Failure initiation statistics of the honeycomb materials

According to the experimental results of Fig. 5, the first failing elements in near-regular / regular honeycombs are gathered in specific locations (especially, near the edges), which is eminently deterministic. The reason is that the elements forming the structures have very similar geometrical and mechanical characteristics so that the boundary artefacts play more decisive role than α and $\underline{V}$ on determining the first element to fail.

Therefore, when the failure initiation statistics of the honeycombs is investigated, the specimens should be irregular enough so that load is uniformly shared within each specimen. Then, the weakest link theory in Eq. (9) can be safely used to estimate the failure initiation statistics of the samples with target scale(s).

In terms of the weakest link theory, the cumulative distributions of honeycomb samples with different $\underline{V}$ can be calculated by using the reference scale, e.g. $\underline{V}_{\text{ref}} = 100$ (i.e. $H/h^0 = 10$) in the present study. It is important to mention that the calculations are conducted for the samples with the same α value. It is observed that the weakest link theory estimates the failure initiation statistics of honeycombs with good accuracy, when α is large enough. As explained above and shown on the left hand-side of Fig. 8, it is inevitable to obtain erroneously estimated distributions for small α.

---Preferred position for Fig. 8---

The weakest link theory is a beneficial statistical tool for estimating the cumulative distributions of the failure initiation for the honeycomb samples with different $\underline{V}$. However, in order to parameterize the estimated distributions and describe them as compact and mathematical expressions, three parameter Weibull distribution of Eq. (10) is substituted into Eq. (9). Once the Weibull parameters are computed for the reference sample of α_{ref} and $\underline{V}_{\text{ref}}$, the distributions for the samples with different $\underline{V}$ but same α_{ref} values are predicted through

$$\text{cdf}(p/p^0, \alpha_{\text{ref}}, \underline{V}) = 1 - \exp\left[-\left(\frac{p/p^0 - \Pi_{\min}^{\text{glob}}}{\lambda}\right)^{\kappa}\right]^{\underline{V}/\underline{V}_{\text{ref}}} \tag{12}$$

where both λ and κ are constant parameters and $\Pi_{\min}^{\text{glob}} \simeq 0.17$ for uniaxial tension case. As an example, the reference samples are chosen as $\alpha_{\text{ref}} = 0.15$ and $\underline{V}_{\text{ref}} = 400$ (i.e. $H/h^0 = 20$) and $\alpha_{\text{ref}} = 0.3$ and $\underline{V}_{\text{ref}} = 400$. The Weibull parameters for the first reference sample distribution are calculated as $\lambda = 0.58$ and $\kappa = 20.67$, while $\lambda = 0.41$ and $\kappa = 10.91$ for the latter one. By substituting these parameters into Eq. (12), cumulative distributions of the target samples are predicted as shown in Fig. 9. The predictions are accurate and in good accordance with the cumulative distributions of the target samples which are obtained through Eq. (8).

---Preferred position for Fig. 9---

6.3. Statistical failure initiation model

In order to form a generic cumulative distribution function, it is necessary to represent λ and κ of Eq. (12) as functions of α instead of a constant term description. As a result of this, the observer can form the statistical failure initiation model based on both α and $\underline{V} = \left(H/h^0\right)^2$ under given external macrostress $\underline{\mathbf{s}}$. By means of this model, (s)he can analyze how many specimens can have failure initiation under the given loading and understand the severity of the condition.

This model can be formed by modifying Eq. (12) so that

$$\mathrm{cdf}(p/p^0, \alpha, \underline{V}) = 1 - \exp\left[-\left(\frac{p/p^0 - \Pi_{\min}^{\mathrm{glob}}}{\lambda(\alpha)}\right)^{\kappa(\alpha)}\right]^{\underline{V}/\underline{V}_{\mathrm{ref}}}. \tag{13}$$

In order to express λ and κ as functions of α as in Eq. (13), values of the parameters are first calculated for the samples with $\underline{V}_{\mathrm{ref}}$. The results are tabulated for the tested loading conditions, i.e. uniaxial tension, combined loading and pure shear in Table 1. Then, the tabulated data lists are represented as third order polynomial functions of α.

---Preferred position for Table 1---

As a result of these operations, $\Pi_{\min}^{\mathrm{glob}}$, $\lambda(\alpha)$ and $\kappa(\alpha)$ of Eq. (13) for the samples with $\underline{V}_{\mathrm{ref}} = 400$ under uniaxial tension, i.e. $\underline{s}_{XX} = s$, $\underline{s}_{XY} = \underline{s}_{YX} = \underline{s}_{YY} = 0$, are obtained as

$$\begin{aligned} &\Pi_{\min}^{\mathrm{glob}} \simeq 0.17, \\ &\lambda(\alpha) = 0.81 - 1.52\,\alpha - 0.39\,\alpha^2 + 3.47\,\alpha^3, \\ &\kappa(\alpha) = 80.5 - 766.6\,\alpha + 3120\,\alpha^2 - 4460\,\alpha^3. \end{aligned} \tag{14}$$

For the samples under combined loading condition $\underline{s}_{XX} = \underline{s}_{XY} = \underline{s}_{YX} = s$, $\underline{s}_{YY} = 0$,

$$\begin{aligned} &\Pi_{\min}^{\mathrm{glob}} \simeq 0.18, \\ &\lambda(\alpha) = 0.82 - 2.7\,\alpha + 6.46\,\alpha^2 - 7.54\,\alpha^3, \\ &\kappa(\alpha) = 99.9 - 1078.4\,\alpha + 4789\,\alpha^2 - 7211\,\alpha^3. \end{aligned} \tag{15}$$

For the samples under pure shear, i.e. $\underline{s}_{XY} = \underline{s}_{YX} = s$, $\underline{s}_{XX} = \underline{s}_{YY} = 0$,

$$\begin{aligned}
&\Pi_{\min}^{\text{glob}} \simeq 0.17, \\
&\lambda(\alpha) = 0.84 - 1.62\,\alpha - 0.13\,\alpha^2 + 5.11\,\alpha^3, \qquad (16) \\
&\kappa(\alpha) = 146.9 - 1708.2\,\alpha + 7657\,\alpha^2 - 11455\,\alpha^3.
\end{aligned}$$

By substituting one of the expressions (14)-(16) above into Eq. (13), the statistical failure initiation model can be formed for the corresponding loading condition. This model can be represented in the macroscopic normal-shear stress space by substituting the variable p/p^0 for $p = \mathbf{s}_{\mathrm{cr}}/\underline{\mathbf{s}}$ of Eq. (6). This substitution is succeeded by calculating the constant scaling terms p^0 for regular honeycombs with $\alpha = 0$, which are $p^0 = 2.64$ for the uniaxial tension, $p^0 = 1.29$ for the combined loading and $p^0 = 1.32$ for the pure shear conditions. Eventually, the statistical failure initiation model for the tested loading conditions is illustrated in Fig. 10.

---Preferred position for Fig. 10---

7. CONCLUSIONS

The current paper introduces a statistical failure initiation model for honeycomb materials. By means of this model, it is aimed to analyze and estimate the failure initiation characteristics quantitatively under given loading and understand the severity of the condition well in advance. The workflow of the model is explained in three stages: micromechanical model, simulation experiments under applied macrostresses and boundary conditions, and analysis of the experiment results. In contrast to the previous studies in the literature, micromechanical models based on the idealized unit cell structure and deterministic analysis approaches are avoided. Instead, a micromechanical model representing the honeycomb material as a heterogeneous medium and statistical analysis tools such as cumulative distribution function, the weakest link theory and Weibull distribution are used. In this respect, the proposed study is expected to advance the current state of art in fields of micromechanics and failure initiation modeling of honeycomb materials.

In this paper, the heterogeneous nature of the honeycomb material is described with independent geometrical parameters which are irregularity α and scale $\underline{V} = \left(H/h^0\right)^2$ and their variations. By means of these parameters, failure initiation characteristics of the honeycombs are investigated. For this purpose, samples based on α and $\underline{V}$ are generated, and experiments are conducted under three different loading conditions which are (I) uniaxial tension, i.e. $\underline{s}_{XX} = s$, $\underline{s}_{XY} = \underline{s}_{YX} = \underline{s}_{YY} = 0$, (II) combined loading, i.e. $\underline{s}_{XX} = \underline{s}_{XY} = \underline{s}_{YX} = s, \underline{s}_{YY} = 0$, (III) pure shear, i.e. $\underline{s}_{XY} = \underline{s}_{YX} = s, \underline{s}_{XX} = \underline{s}_{YY} = 0$. The experiment results are linked to possible failure mechanism(s), e.g. the critical bending moment M_{cr} in this study. In the following step, M_{cr} and the critical macrostress $\mathbf{s}_{\mathrm{cr}}$ causing the first beam to fail are linked to each other with maximization and scaling operations. Then, $\mathbf{s}_{\mathrm{cr}}$ values for the honeycombs with different α and $\underline{V}$ are analyzed by using statistical tools such as the weakest link and Weibull theories. The outcome of the analysis is the generic cumulative distribution function in macroscopic stress space which describes the failure initiation probabilities of the honeycomb materials.

The cumulative distributions for the tested cases show that the failure initiation is more likely for samples with large $\underline{V}$ due to the increasing probabilities for the existence of weak elements inside the specimen. Similarly, the increasing α has a negative effect on the material loading capacity, which results in the weakest element to fail more rapidly than that of a honeycomb material with more regular geometry under the same loading condition. Therefore, increase in both α and $\underline{V}$ yields to higher failure initiation probabilities.

In the literature, similar statistical methods have been successfully used to investigate the failure characteristics of fibrous composites, plain concrete beams, and other quasi-brittle materials such as ceramics and rocks [26-28]. Due to the heterogeneous nature of the examined materials and the similar investigation methods of the previous studies, the proposed statistical model is expected to estimate the failure initiation of the honeycomb materials properly.

ACKNOWLEDGMENTS

The authors gratefully acknowledge the financial support of Multidisciplinary Institute of Digitalisation and Energy (MIDE) through Energy Efficient Wood Processing and Machining Project (E-wood) at Aalto University and the Ministry of Education of Finland through the National Graduate School in Engineering Mechanics. The stimulating discussions on the topic with Dr. Kari Santaoja and proofreading by Ms. Linda Molin are deeply appreciated.

REFERENCES

[1] Gibson LJ, Ashby MF. Cellular solids, structure and properties. Cambridge: Cambridge University Press; 1999.

[2] Gibson LJ, Ashby MF, Schajer GS, Robertson CI. The mechanics of two dimensional cellular materials. Proceedings Royal Society London 1982; A382: 25-42.

[3] Abd El-Sayed FK, Jones R, Burgess IW. A theoretical approach to deformation of honeycomb based composite materials. Composites 1979; 10: 209-214.

[4] Masters IG, Evans KE. Models for the elastic deformation of honeycombs. Composite Structures 1996; 35: 403-422.

[5] Zhu HX, Hobdell JR, Windle AH. Effects of cell irregularity on the elastic properties of 2D Voronoi honeycombs. Journal of the Mechanics and Physics of Solids 2001; 49: 857-870.

[6] Silva MJ, Gibson LJ. The effects of non-periodic microstructure and defects on the compressive strength of two-dimensional cellular solids. International Journal of Mechanical Sciences 1997; 39: 549-563.

[7] Chen C, Lu TJ, Fleck NA. Effect of imperfections on the yielding of two-dimensional foams. Journal of the Mechanics and Physics of Solids 1999; 47: 2235-2272.

[8] Chen C, Fleck NA. Size effects in the constrained deformation of metallic foams. Journal of the Mechanics and Physics of Solids 2002; 50: 955-977.

[9] Yang MY, Hung JS. Failure surfaces for brittle honeycombs with Plateau borders under in-plane biaxial loads. Composite Structures 2006; 72: 512-520.

[10] Karakoç A, Freund J. Effect of geometrical irregularity and scale on failure of wood-like cellular materials. Proceedings of the 22nd Nordic Seminar on Computational Mechanics; 2009: 281-284.

[11] Karakoç A, Freund J. Failure initiation statistics on wood-like cellular structures. Proceedings of the 4th European Congress on Computational Mechanics; 2010. (Available online: https://www.eccm-2010.org/abstract_pdf/abstract_863.pdf.)

[12] Landis E, Vasic S, Davids WG, Parrod P. Coupled experiments and simulations of microstructural damage in wood. Experimental Mechanics 2002; 42: 389-394.

[13] Balawi S, Abot JL. A refined model for the effective in-plane elastic moduli of hexagonal honeycombs. Composite Structures 2008; 84: 147-158.

[14] Karakoç A, Freund J. Effect of geometrical features and scale on failure initiation of wood like cellular material. Proceedings of the 10th Finnish mechanics days; 2009: 534-540.

[15] Jones RM. Mechanics of Composite Materials. Washington D.C.: McGraw-Hill Book Company; 1975.

[16] Karakoç A, Freund J. Experimental studies on mechanical properties of cellular structures using Nomex® honeycomb cores. Composite Structures 2012; 94: 2017-2024.

[17] Suhaimi AB, Saleh AL. Verification of Weibull's theory of brittle fracture to Meranti's timber loaded in tension parallel to the grain. Jurnal Teknologi 2005; 43: 27-34.

[18] Gurvich MR. Strength/size effect for anisotropic brittle materials under a random stress state. Composites Science and Technology 1999; 59: 1701-1711.

[19] Danielsson H. The strength of Glulam beams with holes; A Survey of Tests and Calculation Methods, Report of Structural Mechanics Department of Construction Sciences, Lund, Sweden, 2007.

[20] Tabiei A, Sun J. Analytical simulation of strength size effect in composite materials. Composites: Part B 2000; 31: 133-139.

[21] Weibull W. A statistical theory of the strength of materials. Ingeniorsvetenscaps akademien Handlingar 1939; 151: 1-29.

[22] Vural M, Alkhader M. Mechanical response of cellular solids: Role of cellular topology and microstructural irregularity. International Journal of Engineering Science 2008; 46: 1035–1051.

[23] Fonselius M. Effect of size on the bending strength of laminated veneer lumber. Wood Science and Technology 1997; 31: 399-413.

[24] Bohannan B. Effect of size on bending strength of wood members. Res. Pap. FPL-RP-56. Madison, W1: US Department of Agriculture, Forest Service, Forest Products Laboratory.

[25] Smith I, Landis E, Gang M. Fracture and Fatigue in Wood. John Wiley and Sons; 2003.

[26] Bazant ZP. Size effect aspects of measurements of fracture characteristics of quasibrittle material. Advanced Cement Based Materials 1996; 4: 128–137.

[27] Vorechovsky M. Incorporation of statistical length scale into Weibull strength theory for composites. Composite Structures 2010; 92: 2027-2034.

[28] Mace L, Souche L, Mallet JL. 3D fracture characterization based on geomechanics and geologic data uncertainties. Proceedings of the 9th European Conference on the Mathematics of Oil Recovery; 2004.

Table 1: Weibull parameters λ and κ fitted for the cumulative distributions of the samples with different irregularities α but same $\underline{V}_{\mathrm{ref}} = 400$ (i.e. $H/h^0 = 20$). Tested loading conditions are (I) uniaxial tension, i.e. $\underline{s}_{XX} = s$, $\underline{s}_{XY} = \underline{s}_{YX} = \underline{s}_{YY} = 0$, (II) combined loading, i.e. $\underline{s}_{XX} = \underline{s}_{XY} = \underline{s}_{YX} = s, \underline{s}_{YY} = 0$, (III) pure shear, i.e. $\underline{s}_{XY} = \underline{s}_{YX} = s, \underline{s}_{XX} = \underline{s}_{YY} = 0$.

	Uniaxial tension		Combined loading		Pure shear	
α	λ	κ	λ	κ	λ	κ
0.03	0.76	60.21	0.75	71.7	0.79	102.2
0.15	0.58	20.67	0.54	21.6	0.61	24.2
0.2	0.52	16.31	0.48	18.1	0.55	19.9
0.3	0.41	10.91	0.39	12.7	0.48	14.2

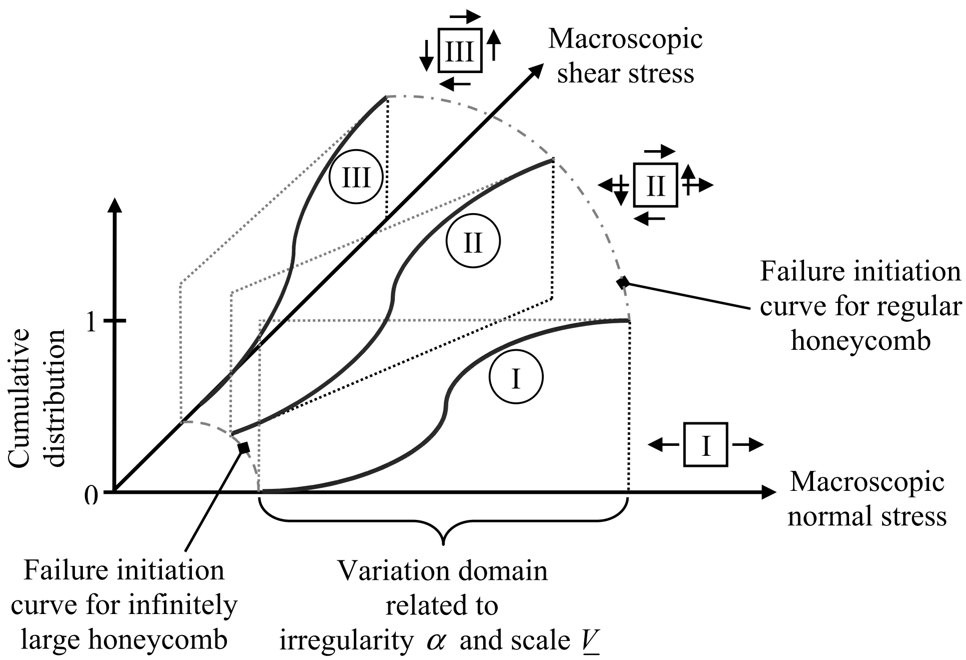

Figure 1: Statistical failure initiation model for honeycomb material.

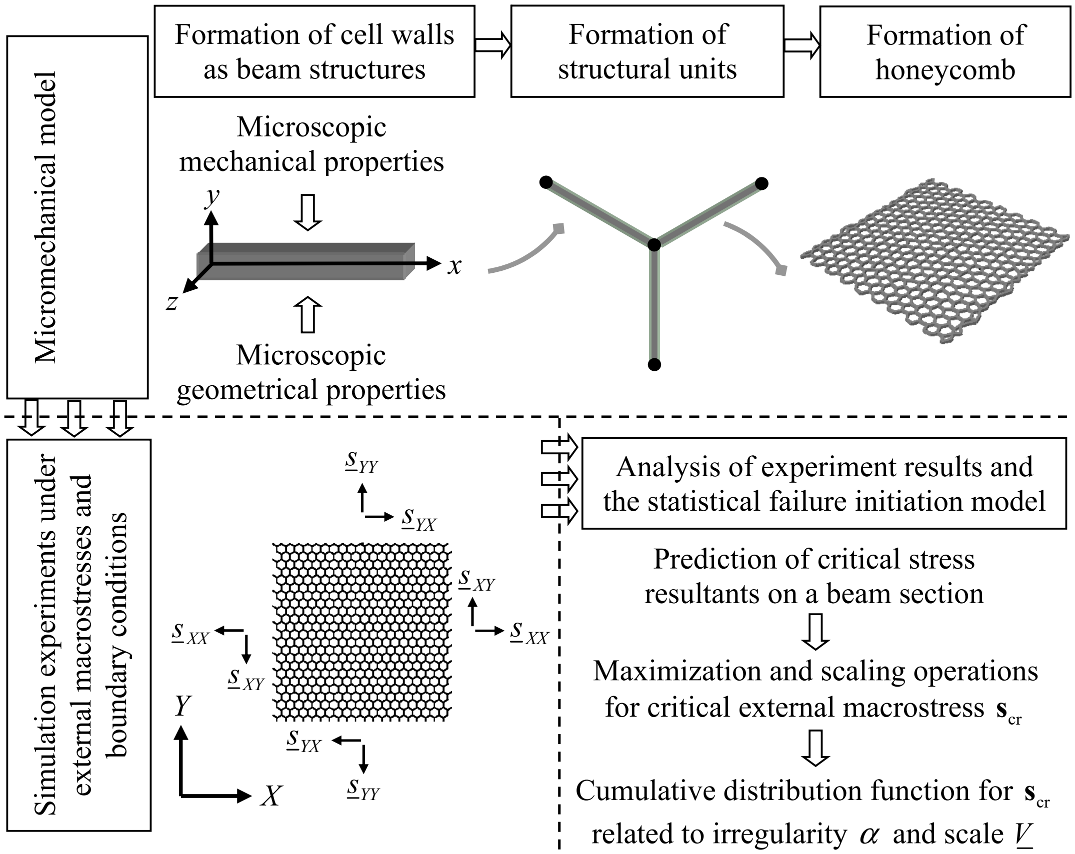

Figure 2: Workflow of the study.

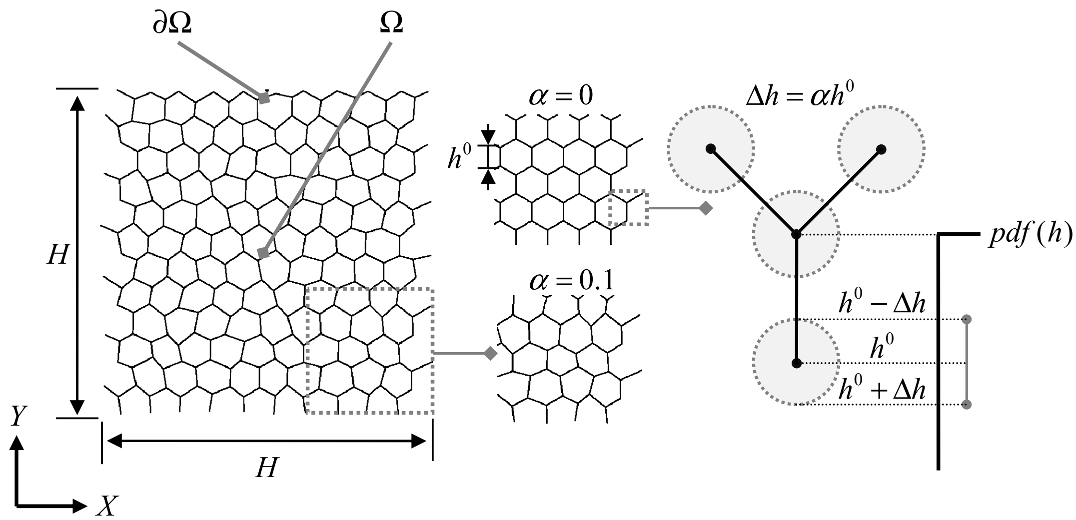

Figure 3: Honeycomb material with independent geometrical variables which are irregularity α and scale $\underline{V} = \left(H/h^0\right)^2$. The specimen and its boundary domains are represented with Ω and $\partial\Omega$, respectively. Here, $pdf(h)$ is the probability density function of cell wall height h for a uniform distribution over the interval $[h^0 - \Delta h, h^0 + \Delta h]$.

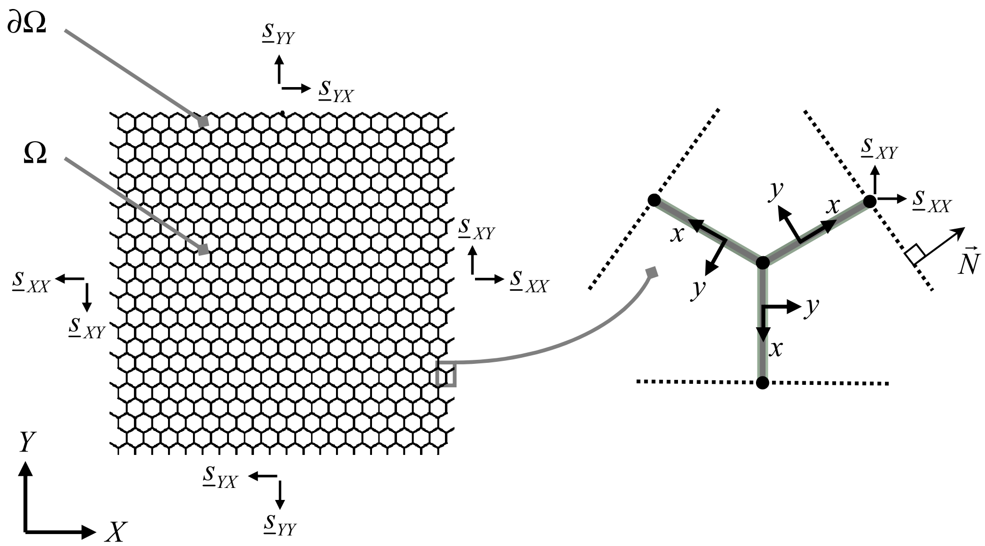

Figure 4: Specimen exposed to external macrostresses. Here, $\underline{s}_{ij}$ for $i, j \in \{X, Y\}$ are the external macrostress components and $\vec{N}$ is the unit surface normal which is parallel to the beam neutral axis.

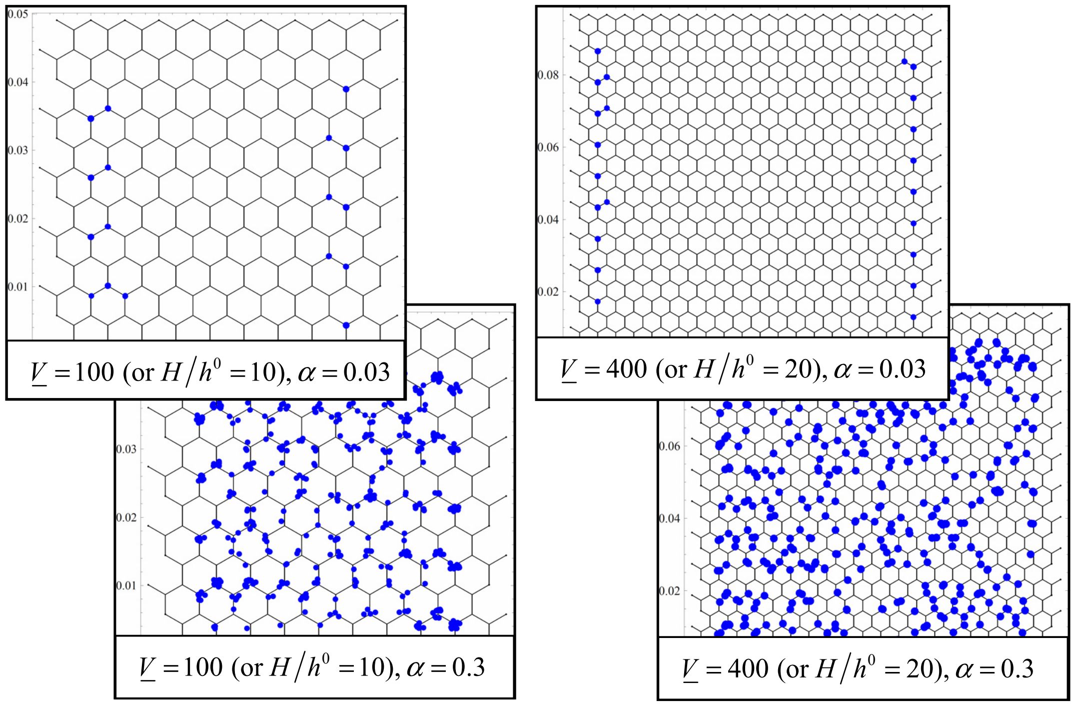

Figure 5: Distributions for the locations of the first failing elements. The scattering of the sites is drawn on regular honeycomb geometry for clarity. Geometries on the right hand-side are scaled down.

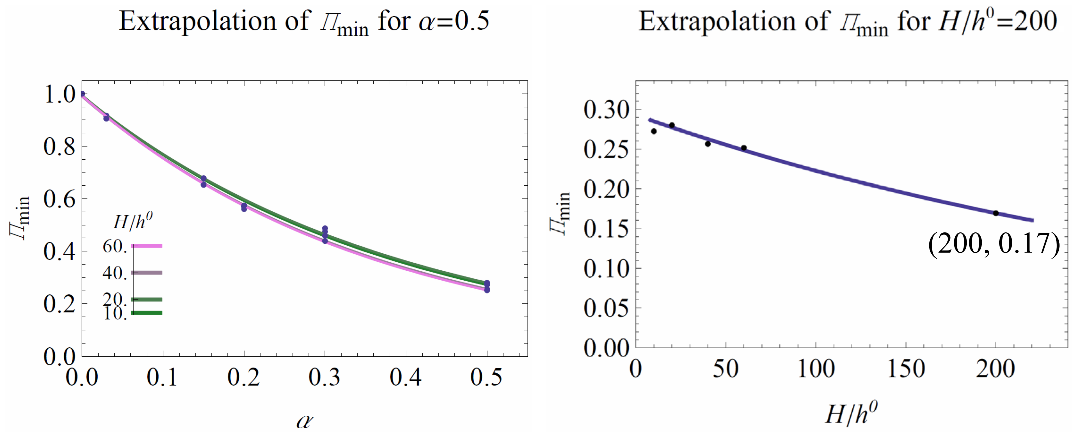

Figure 6: Extrapolation curves used to compute $\Pi_{\min}^{\text{glob}}$ value for uniaxial loading case. The $\Pi_{\min}$ values are first extrapolated to compute the values of $\Pi_{\min}$ for $\alpha = 0.5$ as seen on the left-hand side. The second extrapolation is conducted to obtain the global minimum value $\Pi_{\min}^{\text{glob}}$ for a practically large scale, which is shown on the right-hand side.

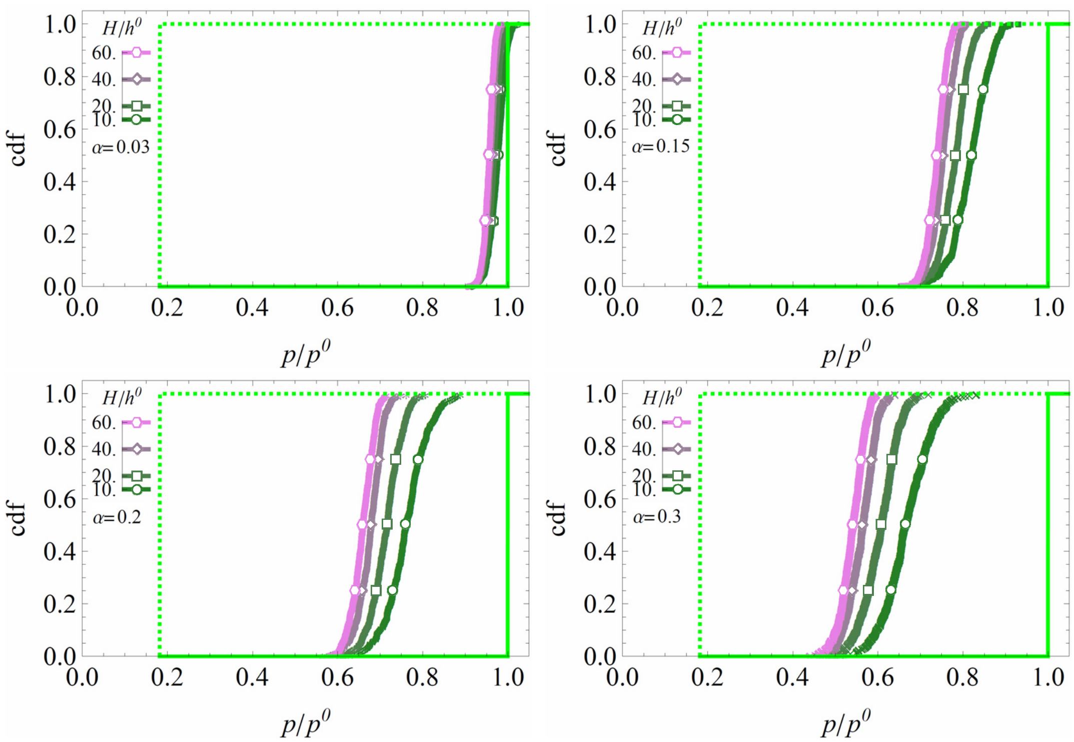

Figure 7: Cumulative distributions for failure initiation of the honeycomb samples with different α and $\underline{V} = \left(H/h^0\right)^2$ under uniaxial tension, i.e. $\underline{s}_{XX} = s$, $\underline{s}_{XY} = \underline{s}_{YX} = \underline{s}_{YY} = 0$. The dashed line on the left hand-side represents the global minimum value $\Pi_{\min}^{\text{glob}} \simeq 0.17$ and the straight line on the right hand-side is the global maximum value $\Pi_{\max}^{\text{glob}} = 1$.

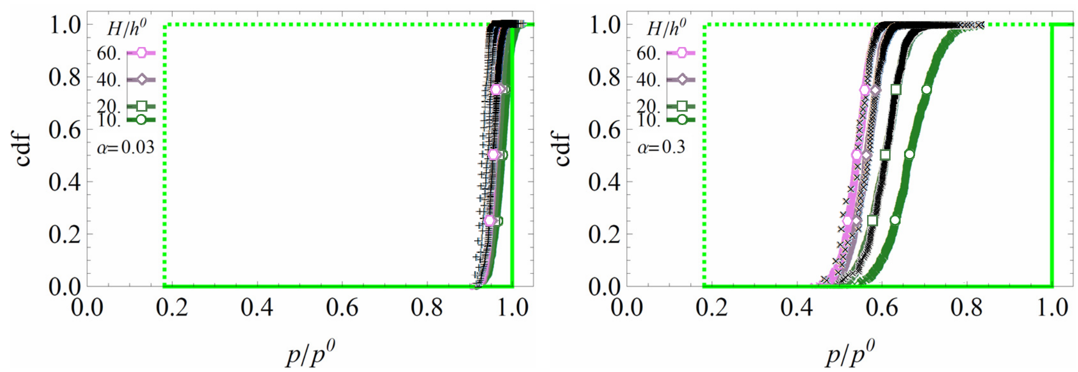

Figure 8: The estimated cumulative distributions for failure initiation of the honeycombs. The black colored points represent the weakest link estimations based on the reference sample scale $\underline{V}_{\text{ref}} = 100$ (i.e. $H/h^0 = 10$).

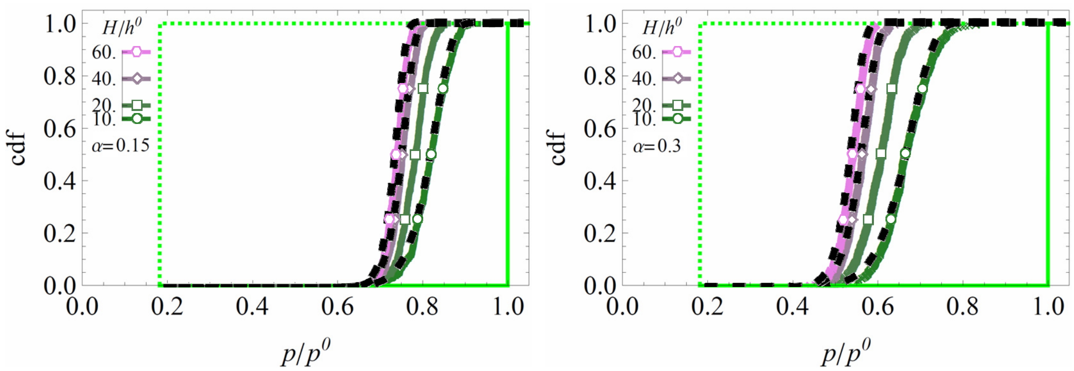

Figure 9: The estimated cumulative distributions obtained based on the reference samples of $\alpha_{\text{ref}} = 0.15$ and $\underline{V}_{\text{ref}} = 400$ (i.e. $H/h^0 = 20$) (left) and $\alpha_{\text{ref}} = 0.3$ and $\underline{V}_{\text{ref}} = 400$ (right). The black dashed lines represent the estimated distributions whereas the reference sample data is shown without dashed lines.

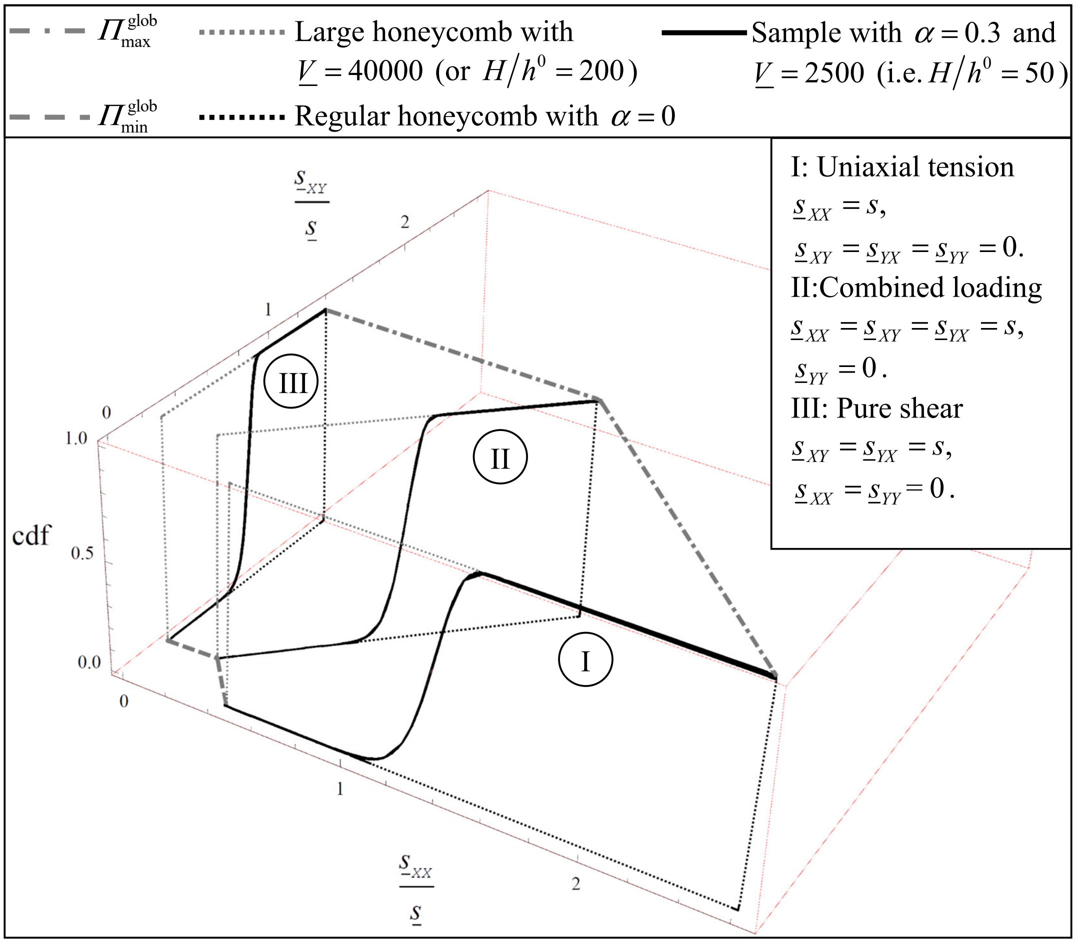

Figure 10: Statistical failure initiation model. Estimated cumulative distributions of samples under various loading conditions are plotted.